# Nanoparticulate ZrO$_2$/SO$_4^{2-}$ Catalyst for Biofuel Production

Sana Labidi[1,*], Mounir Ben Amar[1], Manef Abderrabba[2], Jean-Philippe Passarello[1], Andreï Kanaev[1]

[1]*Laboratoire des Sciences des Procédés et des Matériaux, UPR 3407 CNRS, Institut Galilée, Université Paris13, Sorbonne Paris Cité, 93430 Villetaneuse, France*

[2]*Laboratoire de Physico-chimie Moléculaire, Institut Préparatoire aux Etudes Scientifiques et Techniques, Université de Carthage, Tunisie*

**Abstract:** This study reports on the preparation of zirconia coatings based on monodispersed zirconium-oxo-alkoxy (ZOA) nanoparticles for conversion of free fatty acid (FFA) into biofuel. Monodispersed ZOA nanoparticles of 3.6 nm size were prepared by sol-gel method in a rapid micro-mixing reactor with turbulent fluids flow at 20°C. The ZOA nanopowders obtained after precipitation and nanocoatings deposited on glass beads, after subsequent sulfatation, drying and calcinations, show high catalytic activity towards esterification process. The biofuel yield in esterification of palmitic acid in methanol reached 67% (after t=3.5 hours) on nanopowders while it increases to 98% on nonocoatings.

**Keywords:** Sol-gel, Nanoparticles, Sulfated zirconia, Esterification process.

## INTRODUCTION

Today's challenge is providing power in clean and green way for two mains reasons: (i) inadequacy of fossil fuel and increase of energy demand and (ii) emission of carbon dioxide into atmosphere. This can reinforce the use of biofuel as an alternative clean fuel. The majority of today's commercial production of biofuel is based on homogenous catalysts [1]. The cost of biodiesel production still 1.5 to 3 times higher than conventional petroleum based diesel [2, 3]. Both cost of feedstock and cost of processing are mainly factors that contribute to biofuel production. Concerning feedstock, use of virgin vegetable oils represents 70 to 95% of the total cost of biofuel production [4, 5]. The use of non-edible and waste cooking oils could decrease feedstock cost by 2-3 times [1, 3, 6]. As reported by researchers, heterogeneous catalyst has proved to be cost effective as "green" method [7]. Many research groups have studied the use of different heterogeneous catalysts [3, 8, 9] for biofuel production from different resources of feedstock [2, 6, 10, 11] using methanol or butanol. Base heterogeneous calatyst as zeolite bases calatyst [12-16] and calcium oxide base catalysis [17-19], acid base heterogenous catalyst [7, 20], transition metal bases oxide [21] and biocatalyst (enzymes) [22], were investigated and promising results in biofuel yield of solid heterogenous catalysts have been reported. Economic interests were focused [4-5] and biofuel production costs could be lowered due to use of non-edible and waste cooking oils. To date, several solid acid catalysts have been reported for biofuel synthesis including sulfated zirconia thanks to its high boiling point, strength, toughness and good corrosion resistance in acidic and alkaline environments [23, 24]. It is important to notice that catalytic properties depend on the material structure and morphology. The use of a catalyst of homogenous morphology could enhance its efficiency. A kinetic study of the nucleation-growth process of zirconium-oxo-alkoxy (ZOA) nanoparticles was carried out to control the size and properties of zirconia nanoparticles. The implication of zirconia nanoparticles in esterification of palmitic acid in methanol solvent is studied.

## 1. EXPERIMENT

ZOA nanoparticles were prepared in a sol-gel reactor equipped with rapid micro-mixing as detailed in ref. [25]. The main part of this reactor is a T-mixer of Hartridge and Roughton type with an eccentric reagent injection, which performs at Reynolds numbers typically about $6 \cdot 10^3$ (Re = 4Q$\rho$/$\pi\eta$d, where Q, $\rho$, and $\eta$ are the fluid flow rate, density and dynamic viscosity) [26] and provides turbulent flow of the injected reacting fluids containing (i) zirconium precursor and (ii) water in n-propanol solution at 20°C. The flow is induced by applying ~5 atm pressure of dry nitrogen gas. In present experiments we used zirconium n-propoxide (ZNP) precursor (70% purity, supplied by Interchim), n-propanol solvent (≥99.5% purity, supplied by Sigma-Aldrich) and distilled demineralised and twice-filtered water (syringe filter 0.1 mm porosity PALLs Acrodisc). The residual water content in the alcohols below 0.2% corresponds to the hydrolysis ratio 0.07 in standard reactor conditions: 0.15 mol/L ZNP in 100 mL n-propanol. The reaction medium contained the ZNP

*Address correspondence to this author at the Laboratoire des Sciences des Procédés et des Matériaux, UPR 3407 CNRS, Institut Galilée, Université Paris13, Sorbonne Paris Cité, 93430 Villetaneuse, France; E-mail: labidi.sanatn@yahoo.fr

concentration between 0.100 and 0.150 mol/l and hydrolysis ratio $H=[Zr]/[H_2O]$ between 1.5 and 2.7 was used. The alcohol bottle was kept hermetically closed in a LABstar high-quality glove box workstation MBraun in order to avoid any contamination with atmospheric humidity ($H_2O$ vapour traces below 0.5 ppm). The particle size (2R, nm) and scattered light intensity (I, Hz) were monitored in-situ by respectively dynamic light scattering (DLS) and static light scattering (SLS) methods using an original mono mode optical-fibre probe, 40 mW/640 nm single frequency laser Cube 640-40 Circular (Coherent) and 48 bits 288 channels USB-plugged Photocor-PC2 photon correlator (Photo Cor Instruments). The observation volume defined by a mutual positioning of two monomode optical fibres is sufficiently small ($\sim 10^{-6}$ cm$^3$) to avoid multiple scattering events.

## 2. CATALYST PREPARATION

### 2.1. Preparation of ZOA Nanoparticles

The nucleation of ZOA species, presenting metal oxide core and surface hydroxy (OH) and propoxy (OR) groups, is extremely fast and proceeds on the millisecond timescale following the hydrolysis and condensation reactions (1) and (2):

$$Zr - OR = +H_2 \rightarrow Zr - OH + HOR \qquad (1)$$

$$Zr - OH + HO - Zr \rightarrow Zr - O - Zr + H_2O \qquad (2)$$
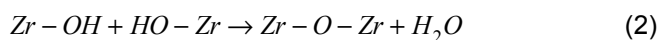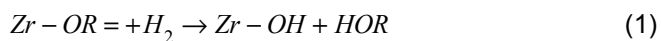
This was confirmed by the light scattering measurements, which evidence the appearance of nanoparticles immediately after the reacting fluids injection into the T-mixer. The nucleation stage is followed by a relatively long period of the particle aggregative growth called the induction period, after which the solution loses stability and ZOA species precipitate. Despite of the seemingly simple and repetitive reaction sequence during the sol-gel synthesis, the nucleated process is complex and involves sequential reactions in the Zr coordination sphere. The produced units depend quite sensibly on the precursor and solvent natures and local reaction conditions (concentrations of species, temperature). The applied turbulent micro mixing homogenises the medium producing point-like reaction conditions, which favour multiple nucleation of fine nanoparticles. The characteristic autocorrelation ACF curve of ZOA sols measured after the fluids micro mixing is shown in Figure **1**.
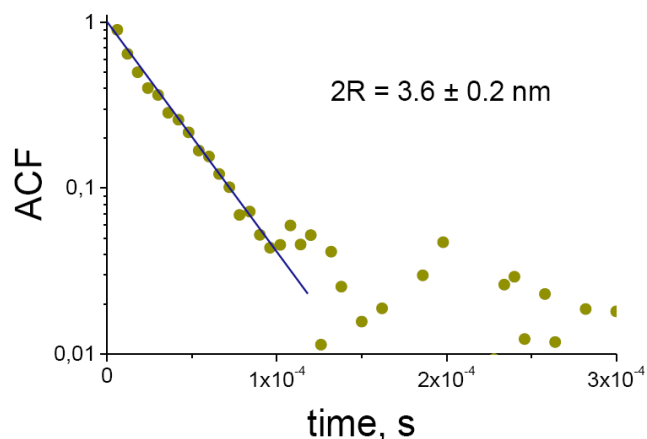


**Figure 1:** ACF of ZOA nanoparticles in n-propanol solution of 0.146M ZNP at H=2.0 (T=20 °C). Solid line shows the exponential fit of the experimental data.

The experimental ACF points can be successfully approximated with one-exponential decay over two decade of magnitude, which indicates a very narrow size distribution. We can conclude about the ZOA particles monodispersity.

As it was shown in previous studies, the growth kinetics of titanium oxo-alkoxy nanoparticles in the sol-gel process depends most sensitively on the hydrolysis ratios H>2.0 [26]. However for low H≤2.0, the nanoparticles exhibit no appreciable aggregation and the colloids remain stable on a timescale of days. The similar tendency has been observed in ZOA nanoparticles [27]. In particularly, in experimental conditions of 0.15 mol/l ZNP and H=2.0±0.1 the nanoparticles' size does not change during ~20 min as shown in Figure **2**. This sequence is sufficient for the deposition process. Based on the obtained information, the ZOA nanoparticulate coatings were realised by the colloid contact with hydrophilic substrates during the time of 20 min.
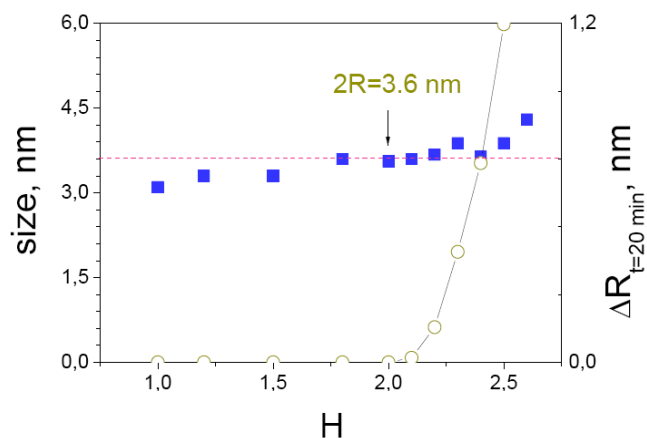


**Figure 2:** Nanoparticles size after fluids injection (left axis) and anter 20 min growth (right axis) in ZNP/n-propanol sol-gel process for different hydrolysis ratios.

## 2.2. Preparation of Sulfated Zirconia

ZOA nanoparticles in solution earlier described were used under nanopowder and nanocoating forms. ZOA nanopowders are obtained directly after precipitation of high H sol (H=2.7) at ambient temperature. After drying at 80°C overnight, ZOA nanopowders were grounded then kept in glovebox. As indicated previously, ZOA nanocoatings on SiO$_2$ beads support are obtained by dip-coating of SiO$_2$ support in ZOA sol. Figure **2** shows that for H=2.0, nanoparticles size is quite stable for more than 48h (horizontal axis in logarithmic scale), thus this situation allows a convenient dip-coating of smallest nanoparticles (R=1.8 nm ± 0.1) on a support. The coated SiO$_2$ beads were filtrated and dried at controlled atmosphere for 4h in glove-box before being kept at 80°C overnight. Nanopowders and nanocoatings were calcinated at 500°C for 4 h. The sulphated ZrO$_2$/SiO$_2$ catalysts were prepared by keeping of respectively 0.2 g of ZrO$_2$ nanopowders and 5g of ZrO$_2$/SiO$_2$ in 50 mL of 1N sulfuric acid solution during 30 min at room temperature. The sulfated nanopowders and nanocoatings were filtrated and finally dried at temperatures between 100 and 150°C during 2 to 24 hours to investigate the influence of the post-sulfatation thermal treatment on catalyst performance.

## 2.3. Catalyst Characterization

It was reported in literature by majority of researchers that sulfatation was frequently applied on amorphous zirconia. In our study, we used sulfatation of calcinated ZrO$_2$. To validate the successful
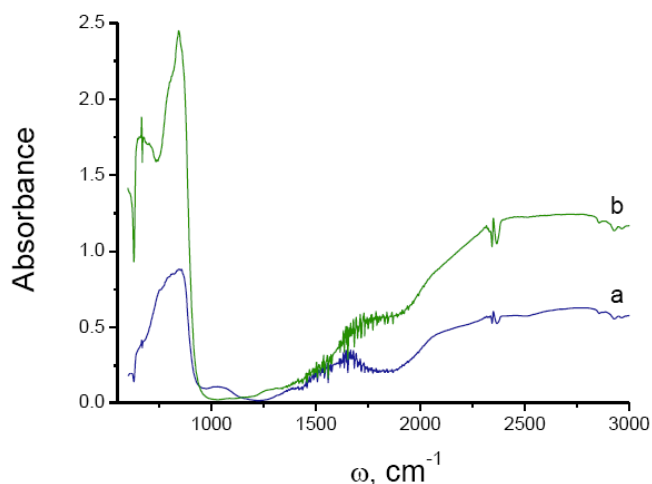
**Figure 3:** DRIFT spectra of pure (**a**) and sulphated (**b**) zirconia powders after thermal treatment at 500°C.

sulfatation, DRIFT analysis was performed on nanopowders. Figure **3** shows the DRIFT spectra of calcinated zirconia nanopowders before (a) and after (b) sulfatation. Figure **3b** depicts vibration bands around 746 and 860 cm$^{-1}$, which are typical to chelating bidentatesulfate ion coordinated to zirconium cation [28]. This result confirms the efficiency of wet impregnation of calcinated ZOA nanopowders. The similar conclusion was drawn after FTIR analysis of the sulfated nanocoatings. The analysis of nanocoatings performed by ICP-OES (Inductive Coupled Plasma - Optical Emission Spectrometry) method resulted in the deposited ZOA mass of 41 mg over 5 g of the supporting material.

## 3. BIOFUEL SYNTHESIS: SYNTHESIS AND OPTIMIZATION OF THE CATALYST

### 3.1. Biofuel Process

The biofuel synthesis considered here consists in the palmitic acid (PA) esterification into methyl palmitate (MP) in methanol solvent according to the following reaction (3):

$$C_{15}H_{31}COOH + CH_3 \Leftrightarrow C_{15}H_{31}COOCH_3 + H_2O \qquad (3)$$
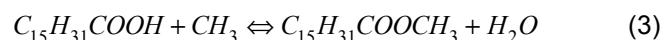
Esterification process was conducted in a well-mixed batch type vessel reactor of 100 ml volume connected to a condenser, in liquid phase with the molar ration R=acid: methanol=1:100 at the atmospheric pressure and temperature 95°C. The moderate experimental conditions were chosen allowing the catalyst response within 8h maximum and low molar ratio to avoid species diffusion problem due to high viscosity. The solid acid catalyst mass of 5g of SO$_4^{2-}$/ZrO$_2$/SiO$_2$ added and the reaction mixture was refluxed with constant stirring. A bulb thermometer was placed in the oil flask to control temperature regulation. The oil flask ensures reactive mixture heating. Since magnetic stirrer was judged to be inappropriate to ensure a good mixing of catalyst with the reactive solution, vessel with condenser were inclined to vertical position by 30°. The sampling (1 mL) of the reactive media was taken periodically each 30 min and cooled down to the room temperature by mixing with 2 mL methanol in a glass tube to bloc reaction. The concentrations of species were determined using Niccolet 6700 Fourrier Transform Infra Red Advanced Gold Spectrometer. The scheme of the biofuel reactor is given in Figure **4**.
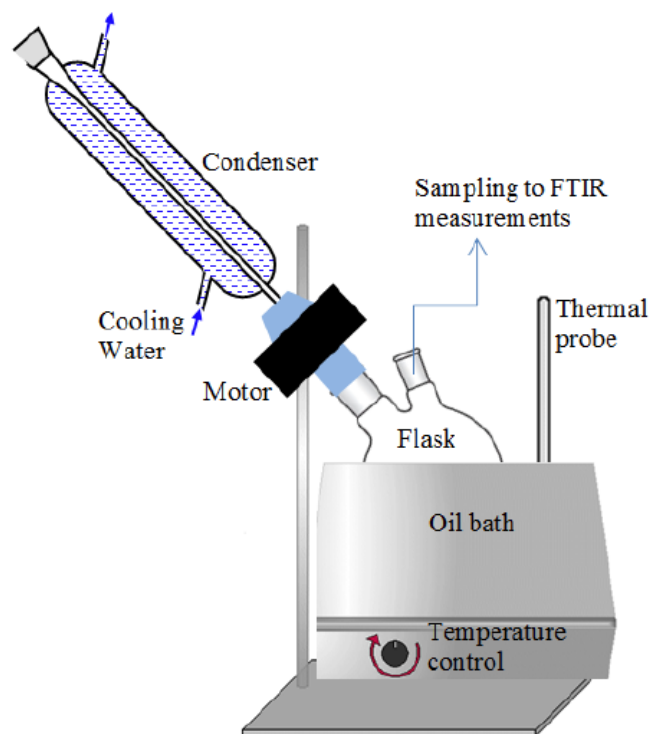
**Figure 4:** Scheme of biofuel process.

### 3.2. FTIR Measurements: Operating Mode

As indicated in the previous paragraph, reagents concentration was determined with in FTIR measurements by using IR light source, DTGS (Deuterated Tri Glycine Sulfate) KBr detector and CaF$_2$ beam splitter. Spectra were measured over a range of wave numbers between 1584 and 2019 cm$^{-1}$, where both reaction species palmitic acid and methyl palmitate have relatively strong absorption bands at respectively 1720 cm$^{-1}$ and 1700-1750 cm$^{-1}$ [29].Outside this range, spectral measurements of reaction products were not possible because of the very strong methanol absorption. For each acquisition, methanol spectrum was taken as background. According to Beer-Lambert law, we have (4):

$$A(\lambda) = K(\lambda) \cdot C \tag{4}$$

where A and K are respectively absorbance and absorption constant at a given wavelength $\lambda$ and C is reagent concentration.

The reference spectra $A(\lambda)$ of palmitic acid (PA) and methylepalmitate (MP) were measured with different concentrations of 0.100, 0.075, 0.050 and 0.025 mol/L in methanol and used to calibrate (4) for the absorption constants $K_i$ of pure reagents PA (Figure **5**) and MP (Figure **6**). In a general case of the mixed reaction

products $i$ in (3) the Beer-Lambert law reflects their concentrations $C_i$ (5):
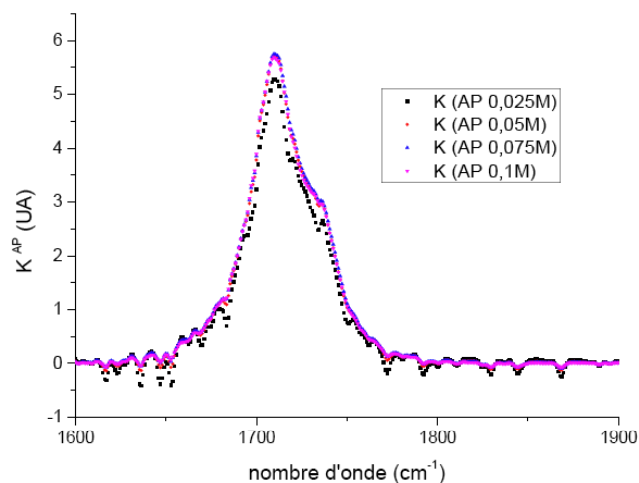


**Figure 5:** Palmitic acid standard spectra for 0.025M, 0.05M, 0.075M and 0.1M concentration of PA in methanol.
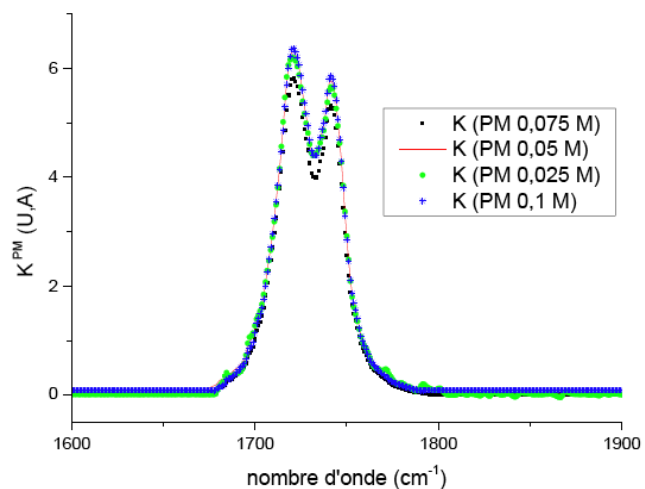


**Figure 6:** Methyl Palmitate standard spectra for 0.025M, 0.05M, 0.075M and 0.1M concentration of PM in methanol.

$$A(\lambda) = \sum_{i=1}^{n} K_i C_i \tag{5}$$

where n=2 in case of our two components system. In the previously mentioned range of wave numbers, the water absorbance was considered as significant and was subtracted by including in the background spectra. Knowing spectral dependence of K for both PA and MP, it becomes possible to calculate intermediate concentrations of both molecules during the esterification process. In order to estimate the precision of this method, mixtures of known concentration (experimental concentrations) of PA and MP were analysed. The spectra of these mixtures are presented

in Figure **7** and fitting of these spectra (to obtain calculated concentrations) using (5) validate the standard error bars ±0.005 mol/L of measured concentrations (Table **1**).
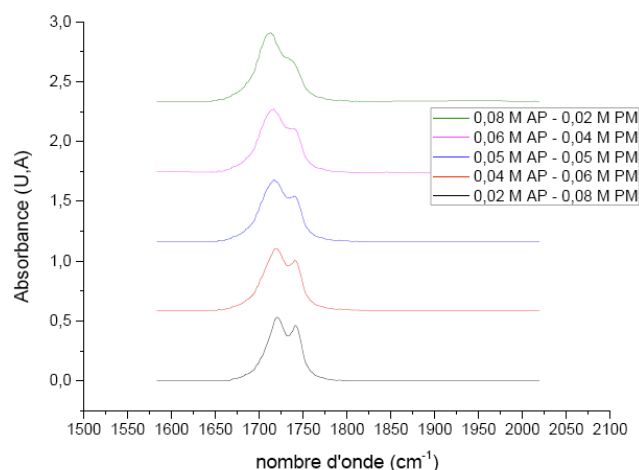


**Figure 7:** Spectra of Methyl Palmitate and palmitic acid mixture with different concentrations.

### 3.3. Biofuel Synthesis: Kinetic Study with FTIR Measurements

The biofuel was synthesized through esterification of palmitic acid in methanol at the molar ratio 1:100 and 65°C. The conversion of palmitic acid (X) was calculated using the following equation (6):

$$X = \frac{C_{MP}^t}{C_{PA}^0} = \frac{C_{MP}^t}{C_{PA}^t + C_{MP}^t} \qquad (6)$$

where, $C_{MP}^t$ and $C_{PA}^t$ are respectively concentrations of methyl palmitate and palmitic acid at time t of the esterification process (t=0 corresponds to the reaction onset) and $C_{AP}^0$, is the initial concentration of palmitic acid. Nanopowders and nonocoatings ZrO$_2$/SO$_4$$^{2-}$

catalysts were employed in the biofuel synthesis reaction obtained after different drying temperatures after wet impregnation with sulfuric acid assummarisedin Table **2**. The conversion yieldsin these experiments are reported in Figure **8**. The series BS17 with catalyst of virgin SiO$_2$ beads and without deposited sulphated zirconia and BS18 (without catalyst) were served as blank series, in which the biofuel yield remained null during 3.5 hours of continuous reaction. The series BS12 and BS14 with nanopowder catalysts, dried at 100°C during 2h and 2h30 respectively, show a notable increase of the biofuel yield comparing to the blank series: within 3h timescale biofuel yield reached 60%. The reproducibility of the biofuel process was successively confirmed. Another series BS20 with catalyst contained 5g of ZrO$_2$/SO$_4$$^{2-}$ deposited on SiO$_2$ beads was realised in similar drying conditions. The biofuel yield in BS20 was increased by 20% comparing with nanopowders and reaches around 80% within 3h of the reaction time. The ZrO$_2$/SO$_4$$^{2-}$/SiO$_2$ catalyst of experimental series BS16 deposited on glass beads and dried at 100°C for 24h resulted in almost complete conversion of palmitic acid within 3.5 hours of the reaction time. In the same time, the biofuel yield decreased dramatically with BS19 series' catalysts, where ZrO$_2$/SO$_4$$^{2-}$/SiO$_2$ beads were dried at 150°C for 24h. The thermal treatment of catalysts affects the biofuel synthesis kinetics through Brønsted and Lewis acid sites number density on sulfated zirconia. Parera and al [24] have shown that the catalytic activity of sulfated zirconia depends on the relative percentage between these two types of acid sites: at higher temperatures, Lewis sites are promoted while Brønsted sites dominate at lower temperatures. In solid acid catalysts, free fat acid is adsorbed on the surface by protonation of carbon in carbonyl group, which is to be attacked by alcohol in liquid phase [30]. This mechanism can be based on Brønsted and Lewis acid sites throughout two mechanisms proposed: a single site (Eley-Rideal, ER model) or dual-site mechanisms (Langmuir-Hinshelwood, LH model). According these two mechanisms, both Brønsted and

**Table 1:   Relative and Standard Error for Spectra Fitting Method**

| Sample | | Experimental Concentrations (mol/L) | Calculated Concentrations (mol/L) | Relative Error | Standard Error (mol/L) |
|---|---|---|---|---|---|
| M1 | PA | 0.02 | 0.0160 | 19.9% | 0.00319 |
| | MP | 0.08 | 0.0767 | 4.1% | 0.00318 |
| M2 | PA | 0.04 | 0.0341 | 14.7% | 0.00501 |
| | MP | 0.06 | 0.0594 | 1.0% | 0.00059 |
| M3 | PA | 0.05 | 0.0474 | 5.2% | 0.00244 |
| | MP | 0.05 | 0.0465 | 7.0% | 0.00327 |
| M4 | PA | 0.06 | 0.0592 | 1.3% | 0.00077 |
| | MP | 0.04 | 0.0383 | 4.3% | 0.00163 |

**Table 2:   Synthesis Conditions of $ZrO_2/SO_4^{2-}$ for Each Experiment**

| Experiment name | Indications for Catalysts Conditions Synthesis |
|---|---|
| BS12 | $ZrO_2/SO_4^{2-}$ nanopowders dried at 100°C for 2h30 |
| BS14 | $ZrO_2/SO_4^{2-}$ nanopowders dried at 100°C for 2h00. |
| BS16 | Loaded $ZrO_2/SO_4^{2-}$ on $SiO_2$ dried at 100°C for 24h00. |
| BS17 | $SiO_2$ beads |
| BS18 | No catalyst |
| BS19 | Loaded $ZrO_2/SO_4^{2-}$ on $SiO_2$ dried at 150°C for 24h00. |
| BS20 | Loaded $ZrO_2/SO_4^{2-}$ on $SiO_2$ dried at 100°C for 2h00. |

Lewis acid sites contribute simultaneously to the esterification reaction. Therefore, the optimal ration between Brønsted and Lewis acid sites would lead to a higher catalytic activity of $ZrO_2/SO_4^{2}$, which seem to correspond to BS16 catalysis obtained after drying at 100°C during 24h after sulfatation.
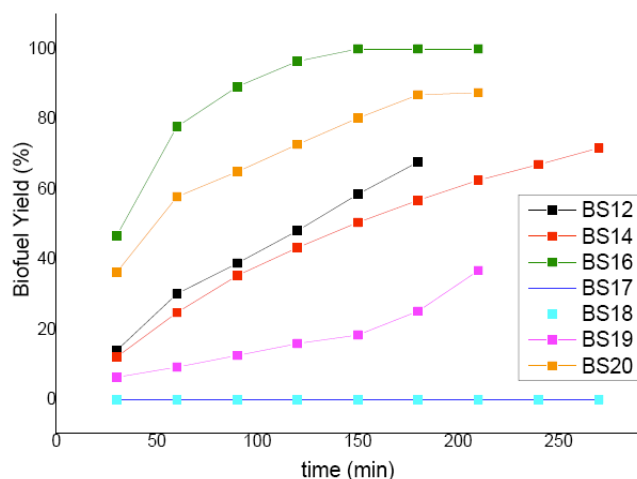


**Figure 8:** Conversion evolution during palmitic acid esterification time for different catalysis ZrO2/SO42- synthesized at different conditions.

## CONCLUSION

The solid acid catalyst based on sulfated nanozirconiapossessing Brønsted and Lewis acid sites was employed in the esterification of palmitic acid in methanol solvent and showed an enhanced activity with 95-99% yield of methyl palmitate at 95°C after 3.5 hours reaction time. The reaction exhibited the first order kinetics with catalyst concentrationsof 1.6wt% in case of nanopowders and 0.005 wt% in case of silica supported nanocoatings. The loaded catalyst may present an attractive alternative to the powders in practical process since pressure drop problem can be avoided.

## ACKNOWLEDGEMENTS

## REFERENCES

[1]     Endalew AK, Kiros Y, Zanzi R. Inorganic heterogeneous catalysts for biodiesel production from vegetable oils. Biomass and Bioenergy 2011; 35: 3787-3809. http://dx.doi.org/10.1016/j.biombioe.2011.06.011

[2]     Canakci M, Sanli H. Biodiesel production from various feedstocks and their effects on the fuel properties. J. Ind. Microbiol. Biothechnol. 2008; 35: 431-41. http://dx.doi.org/10.1007/s10295-008-0337-6

[3]     Di Serio M, Tesser R, Pengmei L, Santacesaria E. Heterogeneous catalysts for biodiesel production. Energy Fuels 2008; 22: 207-17. http://dx.doi.org/10.1021/ef700250g

[4]     Haas MJ, McAloon AJ, Yee WC, Foglia TA. A process model to estimate biodiesel production costs. Bioresour Technol 2006; 97: 671-8. http://dx.doi.org/10.1016/j.biortech.2005.03.039

[5]     Doradoa MP, Cruza F, Palomara JM, López FJ. An approach to the economics of two vegetable oil based biofuels in Spain. Renew Energy 2006; 31: 1231-7. http://dx.doi.org/10.1016/j.renene.2005.06.010

[6]     Zhang Y, Dub MA, McLean DD, Kates M. Biodiesel production from waste cooking oil: 2. Economic assessment and sensitivity analysis. Bioresour Technol 2003; 90: 229-40. http://dx.doi.org/10.1016/S0960-8524(03)00150-0

[7]     Tanabe K, HoÈlderich WF. Industrial application of solid acid-base catalysts. Appl. Catal. A, 181 (1999): 399-434. http://dx.doi.org/10.1016/S0926-860X(98)00397-4

[8]     Shi W, He B, Ding J, Li J, Yan F, Liang X. Preparation and characterization of organic-inorganic hybrid membrane for biodiesel production. Bioresour Technol 2010; 101: 1501-5. http://dx.doi.org/10.1016/j.biortech.2009.07.014

[9]     Kiss AA, Omota F, Dimian AC, Rothenberg G. The heterogeneous advantage: biodiesel by catalytic reactivedistillation. Top Catal 2006; 40: 141-50. http://dx.doi.org/10.1007/s11244-006-0116-4

[10]    CCCM. Silva, NFP Ribeiro, MMVM. Souza, DAG. Aranda. Biodiesel production from soybean and methanol using

hydrotalcites as catalyst. Fuel Process Technol 2010; 9: 205-10.
http://dx.doi.org/10.1016/j.fuproc.2009.09.019

[11] KH. Chung, BG. Park. Esterification of oleic acid in soybean oil on zeolite catalysts with different acidity. J Ind Eng Chem2009; 15: 388-92.
http://dx.doi.org/10.1016/j.jiec.2008.11.012

[12] BO. Aderemi, BH. Hameed. Alum as a heterogeneous catalyst for transesterification of palm oil Appl Catal A 2009; 370: 54-8.
http://dx.doi.org/10.1016/j.apcata.2009.09.020

[13] KH. Chung, DR Chang, BG. Park. Removal of free fatty acid in waste frying oil by esterification with methanol on zeolite catalysts Bioresour Technol 2008; 99: 7438-43.
http://dx.doi.org/10.1016/j.biortech.2008.02.031

[14] A. Brito, ME. Borges, N. Otero. Zeolite Y as a heterogeneous catalyst in biodiesel fuel production from used vegetable oil. Energy Fuels 2007; 21: 3280-3.
http://dx.doi.org/10.1021/ef700455r

[15] Q. Shu, B. Yang, H. Yuan, S. Qing, G. Zhu. Synthesis of biodiesel from soybean oil and methanol catalyzedby zeolite beta modified with La$^{3+}$. Catal Commun 2007; 8: 2159-65.
http://dx.doi.org/10.1016/j.catcom.2007.04.028

[16] M. Sasidharan, R. Kumar. Transesterification over various zeolites under liquid-phase conditions. J Mol.Catal A Chem 2004; 210: 93-8.
http://dx.doi.org/10.1016/j.molcata.2003.08.031

[17] BY. Cho, G. Seo, DR. Chang. Transesterification of tributyrinwith methanol over calcium oxide catalyst prepared from varies precursors. Fuel Process Technol 2009; 90: 1252-8.
http://dx.doi.org/10.1016/j.fuproc.2009.06.007

[18] MCG. Albuquerque, I. Jiménez-Urbistondo, J. Santamaría-Gonzàlez, J.M. Mérida-Robles, R. Moreno-Tost, E. Rodríguez-Castellón, *et al*. CaO supported on mesoporoussilicas as basic catalysts for transesterification reactions. Appl Catal A 2008; 334: 35-43.
http://dx.doi.org/10.1016/j.apcata.2007.09.028

[19] G. Arzamendi, I. Campo, E. Arguinarena, M. Sanchez, M. Montes, LM. Gandia. Synthesis of biodiesel with heterogeneous NaOH/alumina catalysts: comparison with homogeneous NaOH Chem Eng J 2007; 134: 123-30.
http://dx.doi.org/10.1016/j.cej.2007.03.049

[20] TA. Peters, NE. Benes, A. Holmen, JTF. Keurentjes. Comparison of commercial solid acid catalysts for the esterification of acetic acid with butanol. Appl Catal A 2006; 297: 182-8.
http://dx.doi.org/10.1016/j.apcata.2005.09.006

[21] ST. Kolaczkowski, UA. Asli, MG. Davidson. A new heterogeneous ZnL$_2$catalyst on structured support forbiodiesel production Catal Today 2009; 147: S220-4.
http://dx.doi.org/10.1016/j.cattod.2009.07.060

[22] (37) MK. Lam, KT. Lee, AR. Mohamed. Homogeneous, heterogeneous and enzymatic catalysis for transesterification of high free fatty acid oil (waste cooking oil) to biodiesel: a review. Biotechnol Adv 2010; 28: 500-18.
http://dx.doi.org/10.1016/j.biotechadv.2010.03.002

[23] VG. Deshmaneet, YG. Adewuyi. Mesoporousnanocrystalline sulfated zirconia synthesis and its application for FFA esterification in oils, Appl Catal A: General 462-463 (2013) 196-206
http://dx.doi.org/10.1016/j.apcata.2013.05.005

[24] JM. Parera, Promotion of zirconia acidity by addition of sulfate ion, Catal Today 1992; 15: 481-490
http://dx.doi.org/10.1016/0920-5861(92)85013-C

[25] M. Rivallin, M. Benmami, A. Kanaev, A. Gaunand, Sol-gel reactor with rapid micromixing: modelling and measurements of titanium oxide nano-particles growth, Chem Eng Res Des 2005; 83: 67-74.
http://dx.doi.org/10.1205/cherd.03073

[26] R. Azouani, A. Michau, K. Hassouni, K. Chhor, JF. Bocquet, J.-L. Vignes, A.Kanaev.Elaboration of pure and doped TiO$_2$ nanoparticles in sol–gelreactor with turbulent micromixing: Application tonanocoatings and photocatalysis. I Chem E. 2010; 88: 1123-1130.
http://dx.doi.org/10.1016/j.cherd.2009.10.001

[27] R. Azouani, A. Soloviev, M. Benmami, K. Chhor, JF. Bocquet, A. Kanaev,Stability and growth of titanium-oxo-alcoxy Ti$_x$O$_y$ (O$^i$Pr)$_z$ clusters, J Phys Chem C 2007; 111: 16243-16248.
http://dx.doi.org/10.1021/jp073949h

[28] S. Labidi, Z. Jia, M. Ben Amar, K. Chhor and A. Kanaev, Phys. Chem. Chem. Phys. Nucleation and growth kinetics of zirconium-oxoalkoxy nanoparticles 2015; 17: 2651-2659.

[29] H. Matsuhashi, M. Tanaka, H. Nakamura, K. Arata, Appl. Catal.A, Formation of acid sites in ordered pores of FSM-16 by modification with sulfated zirconia 2001; 208: 1-5.

[30] A Handbook of spectroscopic data chemistry (UV, IR, PMR, 13CNMR, and Mass Spectroscopy), Mistry B.D, ISBN 978-81-89473-86-0, 2009, 38-39.

[31] Kulkarni MG, Gopinath R, Meher LC, Dalai AK. Solid acid catalyzed biodiesel production by simultaneous esterification and transesterification. Green Chem 2006; 8: 1056-62.
http://dx.doi.org/10.1039/b605713f